Development 133, 1113-1123 (2006) doi:10.1242/dev.02283

# Direct visualization of nucleogenesis by precerebellar neurons: involvement of ventricle-directed, radial fibre-associated migration

**Daisuke Kawauchi[1,2,*], Hiroki Taniguchi[3,†], Haruyasu Watanabe[1], Tetsuichiro Saito[4,*] and Fujio Murakami[1,‡]**

Nuclei are aggregates of neurons distributed in the central nervous system and are fundamental functional units that share anatomical and physiological features. Despite their importance, the cellular basis that leads to nucleogenesis is only poorly understood. Using exo utero electroporation with an enhanced yellow fluorescent protein (EYFP) gene, we show that the precerebellar neurons derived from the lower rhombic lip (lRL) undergo multiple migration steps to form nuclei. After the unilateral transfer of *EYFP* to the lRL of embryonic day 12.5 mice, EYFP-labelled neurons migrate tangentially from the lRL in two distinct streams, one towards the ventral metencephalon and the other towards the ventral myelencephalon. These neurons cross the ventral midline and then become radially directed. Labelled neurons in the tangential migratory streams form contralateral clusters in the external cuneate nucleus (ECN) and lateral reticular nucleus (LRN) in the myelencephalon, and bilateral clusters in the pontine grey nucleus (PGN) and reticulotegmental nucleus (RTN) in the metencephalon. Before forming the clusters, EYFP-labelled neurons begin to migrate radially towards the ventricle in close apposition to nestin-positive radial fibres, and then they aggregate as they detach from the fibres. Inhibition of cadherin function in ECN and LRN progenitors caused ipsilateral formation of the ECN and LRN, implying that the transition of their migration from tangential to radial involves a cell-intrinsic mechanism. These observations suggest that nucleogenesis of precerebellar neurons is a result of multi-phasic migration, and that ventricle-directed radial glia-guided migration is a key step for nucleogenesis.

**KEY WORDS: Neuronal migration, Precerebellar neurons, Nucleogenesis, In vivo electroporation, Midline crossing, Ventricle-directed migration, Mouse**

## INTRODUCTION

In the vertebrate central nervous system, there are important functional units called layers and nuclei. Structures such as the cerebral cortex and the hippocampus have a layered neuronal organization, whereas nuclei are aggregates of neurons dispersed throughout the central nervous system. Neurons in nuclei and those in some layers have common physiological and anatomical features, including projections to and from other functional units, which is essential for brain functions.

Mechanisms in the development of stratified structures have been well documented (reviewed by Hatten, 1999; Marin and Rubenstein, 2003; Komuro and Yacubova, 2003; Bielas et al., 2004). However, much less is understood about nucleogenesis. Recently, it has been proposed, in the midbrain, that periodic patterns of molecularly distinct stripes that appear to be induced by sonic hedgehog and FGF8 play an important role in the formation of the red nucleus and oculomotor nucleus (Agarwala and Ragsdale, 2002). Concentration-dependent induction by morphogens such as sonic hedgehog and FGF8 may explain the formation of laminated or striped structures (reviewed by Goulding and Lamar, 2000), but cannot fully explain the emergence of discretely distributed nuclei.

Neuronal migration is another potential factor in nucleogenesis and its role is well established in the formation of stratified structures. In the cerebral cortex, for example, excitatory neurons that are born in the ventricular zone migrate along the radial glial cells that span the cerebral wall (Rakic, 1972; Hatanaka and Murakami, 2002) (reviewed by Kriegstein and Noctor, 2004) and settle in specific lamina in a birthdate-dependent manner (Rakic, 1974). Later-born cells migrate past earlier-born cells, forming inside-out laminated structures that lie parallel to the pial surface (Angevine and Sidman, 1961; Berry and Rogers, 1965).

Here, we examined how neuronal migration leads to establishment of nuclei, focusing on the hindbrain where clear nuclear organization exists. A number of studies have addressed the migration of hindbrain neurons and several genes affecting their migration have been identified (reviewed by Hatten, 1999; Wingate 2001; Chandrasekhar, 2004; Sotelo, 2004). Yet, cellular basis for nucleogenesis is still poorly understood. Specifically, how neurons with common properties accumulate in a defined position remains unknown. We have chosen mossy fibre-projecting precerebellar (PC) nuclei as a model, because their origin and development is well documented (Altman and Bayer, 1997; Rodriguez and Dymecki, 2000; Wang et al., 2005). Previous studies have suggested that neurons of the PC nuclei are derived from the lower rhombic lip (lRL), the germinal neuroepithelium surrounding the alar recess of the fourth ventricle (Harkmark, 1954; Taber-Pierce, 1966; Tan and Le Douarin, 1991; Altman and Bayer, 1997; Rodriguez and Dymecki, 2000; Wang et al., 2005), and migrate circumferentially.

[1]Laboratory of Neuroscience, Graduate School of Frontier Biosciences, Osaka University, Suita, Osaka 565-0871, Japan. [2]SORST, Japan Science and Technology, Kawaguchi, Saitama 332-0012, Japan. [3]Division of Behavior and Neurobiology, National Institute for Basic Biology, Myodaiji-cho, Okazaki 444-8585, Japan. [4]Department of Development and Differentiation, Institute for Frontier Medical Sciences, Kyoto University, Kyoto 606-8507, Japan.

*Present address: Department of Developmental Biology, Graduate School of Medicine, Chiba University, Chiba 260-8670, Japan
†Present address: Cold Spring Harbor Laboratory, Beckman 220, One Bungtown Road, Cold Spring Harbor, NY 11724, USA
‡Author for correspondence (e-mail: murakami@fbs.osaka-u.ac.jp)

**Accepted 13 January 2006**

Although these studies examined the origin, migratory route and the fate of alar plate-derived neurons, the cellular processes leading to nucleogenesis were not established, owing to the lack of techniques that allow in vivo visualization of individual neurons migrating from a specific site of the neural tube. To clarify these issues, we introduced the enhanced yellow fluorescent protein (EYFP) gene into the lRL of mouse embryos and visualized migration and nucleogenesis of mossy fibre-projecting PC neurons.

## MATERIALS AND METHODS

### Animals

ICR mice were obtained from CLEA JAPAN (Tokyo). The day that the vaginal plug was detected was considered embryonic day (E) 0.5. Pregnant mice were deeply anesthetized with pentobarbital (50 mg/kg), and embryos were removed from the dams. All experiments followed the Osaka University Guidelines for the Welfare and Use of Laboratory Animals.

### Expression vectors

The whole coding regions for *EYFP* (Clontech) and *Venus* (Nagai et al., 2002) were cloned into the pCAGGS vector (Niwa et al., 1991), yielding pCAG-EYFP (Saba et al., 2003) and pCAG-Venus, respectively. For inhibition of cadherin function, pCAG-Ncad(t) that carried a gene encoding an intracellular domain of *N-cadherin* fused to *enhanced green fluorescent protein* (*EGFP*) was prepared (H.T, D.K., K. Nishida and F.M., unpublished). A vector carrying *Venus* was kindly provided by Dr A. Miyawaki (BSI, Riken).

### Labelling of PC neurons by exo utero electroporation

Exo utero electroporation was performed as previously described (Saba et al., 2003) (Fig. 1A) with some modifications. In brief, plasmids were diluted in 0.01% Fast Green or Indigo carmine (final concentration, ~2 μg/μl) to monitor the injection and was injected into the fourth ventricle of an embryo exposed by cutting the uterine wall.

Three electric pulses (20 V, 50 ms) were applied with an electroporator (ECM830, BTX). Plasmids were unilaterally introduced into the lRL of E12.5 mouse embryos. The vector, once incorporated into the ventricular neuroepithelial cells, should be present in their descendents. Embryos with unilaterally labelled lRL were selected by epifluorescence microscopy (SZX12, Olympus). Hindbrains were removed from these embryos and immersed in 4% paraformaldehyde in 0.1 M sodium phosphate buffer at pH 7.4 (4% paraformaldehyde) overnight at 4°C. The fixed hindbrains were imaged using a cooled CCD camera equipped with epifluorescence illumination (VB-G25, Keyence). Alternatively, the hindbrains were embedded in OCT compound (Sakura Finetechnical) after immersion in 30% sucrose in PBS. Sections (18-20 μm) were cut on a cryostat (HM-500, Zeiss) and mounted on slides (12-550-15, Fisher Scientific). The distribution of EYFP- or Venus-labelled cells was analysed using a confocal microscope (TCS SP2 AOBS, Leica).

### In situ hybridization

The vector carrying the *Mbh2* gene (AB043980; GenBank) was linearized and used as a template for RNA synthesis. An RNA probe for *Mbh2* was subsequently synthesized using a digoxigenin (DIG)-11-UTP mixture (Roche) and T3 or T7 RNA polymerase (Roche), and purified with Quick spin columns (Roche).

Cryosections from the hindbrain of E14.5-18.5 mouse embryos prepared as described above were dried at 50°C for 3-5 hours. The dried sections were refixed in 4% PFA for 5 minutes, and then treated with 0.3% hydrogen peroxide in PBS for 30 minutes. After acetylation with 0.25% acetic anhydride in 0.1 M triethanolamine, the sections were probed with DIG-labelled *Mbh2* cRNA probes (2 ng/μl) in hybridization solution (50% formamide, 5× SSPE, 5% SDS, 200 μg/ml yeast tRNA) for 16 hours at 70°C. After washing, the sections were treated with RNase A (20 μg/ml; QIAGEN) for 1 hour at 37°C. Samples were reacted with a peroxidase-conjugated anti-DIG antibody (1:200, Roche) in Tris-buffered saline containing 1% blocking reagent (Roche). The tyramide signal amplification system (PerkinElmer Life Sciences) was then applied following the manufacturer's instructions.

### Immunostaining

A rabbit polyclonal anti-green fluorescent protein (GFP) antibody (1:1000, Molecular Probes) was used on sections of EYFP- and Venus-labelled hindbrain tissues. To detect EYFP/Venus denatured by in situ hybridization procedures, the sections were reacted with the anti-GFP antibody for 2 hours at room temperature. After a washing with 0.1% Tween-20 in PBS, the signal was visualized with an Alexa488-conjugated anti-rabbit IgG antibody (Molecular Probes).

Radial glial fibres were identified using an anti-nestin antibody (rat401) (Hockfield and McKay, 1985). The antibody was diluted 1:5 in 0.3% Triton-X100 in PBS (PBST) and applied to 30-40 μm sections that had been pretreated with 0.3% hydrogen peroxide in PBS for 30 minutes at room temperature. After overnight incubation at room temperature, sections were rinsed in 0.3% PBST and reacted with biotinylated anti-rat IgG antibody (1:200, Jackson ImmunoRes). Sections were then treated with Vectastain Elite ABC kit (PK-6100, Vector) followed by the tyramide signal amplification method as described above.

### BrdU labelling study

For birthdating studies, intraperitoneal injections with 5′-bromo-2′-deoxyuridine (BrdU) (Sigma; 5 mg/ml in sterile saline) were made in *EYFP*-electroporated pregnant mice at 50 mg/kg body weight to label embryos at E12.5, E13.5 and E14.5 ($n$=5 at each stage). To detect incorporated BrdU, 25 μm transverse sections of the pons were prepared. These sections were incubated in 4 N HCl for 45 minutes, rinsed in 0.2% PBST and reacted with a rat monoclonal anti-BrdU antibody (Cat# OBT-0030, 1:200, Oxford Biotechnology) for 2 hours at room temperature. After extensive washing with 0.2% PBST, the sections were incubated with a biotinylated anti-rat IgG antibody (1:200, Jackson ImmunoRes) for 2 hours at room temperature followed by visualization with Alexa594-conjugated streptavidin. Subsequently, the EYFP protein that had been denatured by the HCl treatment was stained with an anti-GFP antibody.

Captured images were thresholded for quantification using Leica confocal software (Ver 2.61). The total number of EYFP-labelled cells ($N_{total}$) and the number of EYFP-labelled cells that were also positive for BrdU ($N_{BrdU}$) were counted in the entire PGN/RTN on the side of the contralateral to the DNA injection. The ratio of BrdU-positive cells to all EYFP-labelled cells ($N_{BrdU}/N_{total}$) was calculated.

### Electron microscopy

The hindbrain of E15.5 mice was removed and immersed in a fixative consisting of 4% PFA (TAAB) and 0.2% glutaraldehyde (EM Science) in 0.1 M sodium cacodylate (Nacalai Tesque). The preparation was further fixed in 2% glutaraldehyde at 4°C overnight followed by postfixation in 2% OsO4 and then subjected to conventional procedures of electron microscopy. Thin sections were cut coronally. The plane of section was carefully chosen so that radially running fibres can be observed in the sections. Electron microscopy was carried out in Hanaichi Denshi Kenbikyo Laboratory.

## RESULTS

After electroporation of vectors to the lRL at E12.5, embryos were allowed to survive for 2-6 days outside the uterine wall. Brain development in such embryos was indistinguishable from that seen in normal embryos. Analysis of the lRL in all brains showed that unilateral labelling was successful.

### PC neurons can be specifically labelled in vivo by exo utero electroporation of EYFP

The neurons of the external cuneate nucleus (ECN) and the lateral reticular nucleus (LRN) are generated earlier (E10.5-13.5) than those of the pontine grey nucleus (PGN) and reticulotegmental nucleus (RTN) (E11.5-16.5) (Taber-Pierce, 1973). The former migrate circumferentially to give rise to the posterior extramural migratory stream (PEMS), while the latter take a more anteriorly oriented route to form the anterior extramural migratory stream (AEMS) (Altman and Bayer, 1987a; Altman and Bayer, 1987b). Direct visualization of lRL-derived cells largely confirmed these

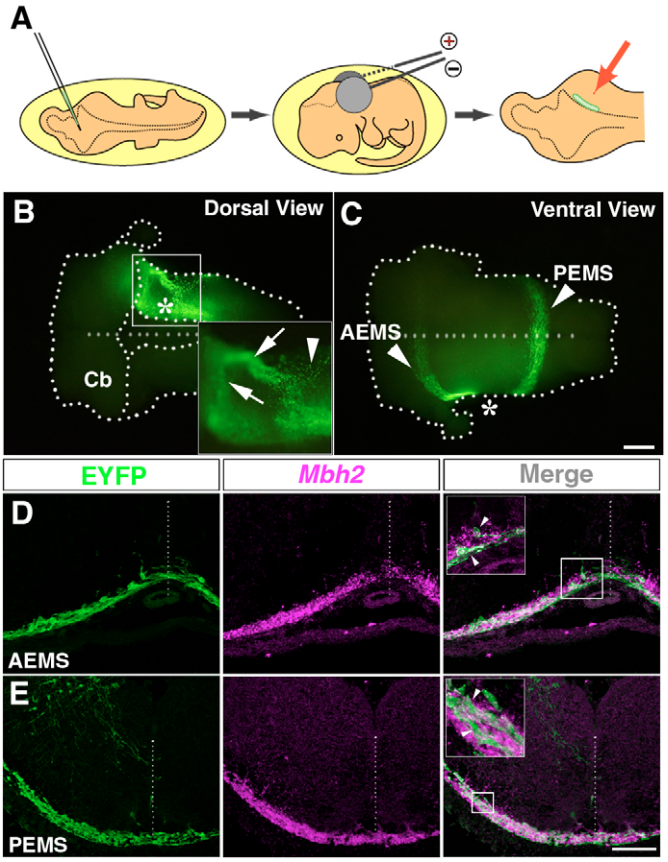


**Fig. 1. In vivo labelling of lRL-derived PC neurons by exo utero electroporation of *EYFP*.** (**A**) Diagram outlining the method. Following injection of a plasmid carrying *EYFP* or *Venus* (left panel), electric pulses were applied. Red arrow indicates an EYFP-transfected region. (**B,C**) Dorsal (B) and ventral (C) views of the hindbrain (outlined) that was electroporated with *EYFP* at E12.5 and fixed at E14.5. There are two streams of labelled cells, the AEMS and PEMS (arrowheads in C). The cells in the AEMS take two separate routes (arrows in the inset of B). Because neurons in the PEMS begin their migration earlier, most labelled cells therein were located ventrally, leaving few cells behind (arrowhead in the inset of B). Rostral is towards the left. Asterisks show the *EYFP*-transfected side, the broken horizontal lines show the midline. (**D,E**) Transverse sections of *EYFP*-introduced embryos immunostained for EYFP (green, left panel), after *Mbh2* in situ hybridization (purple, middle panel). The left, middle and right panels in D and E show the same field of view of metencephalon (D) and myelencephalon (E). In both, EYFP-labelled migrating cells expressed *Mbh2* (arrowheads in insets of D and E). Broken vertical lines show the midline. Dorsal is upwards and *EYFP*-transfected side is towards the left. Cb, cerebellum. Scale bars: 500 μm in B and C; 250 μm in the inset of B; 100 μm in D; 200 μm in E; 55 μm for right panel insets in D,E.

previous findings (Fig. 1B,C; $n$=16). Fig. 1B shows the dorsal view of the E14.5 mouse hindbrain expressing EYFP in the right lRL. A rostroventrally directed stream of EYFP-labelled cells emerged from the lRL. Migrating cells that formed the PEMS were barely visible in the dorsal hindbrain at this stage, perhaps because they had already emigrated (arrowhead in the inset of Fig. 1B). Indeed in the ventral view, neurons in the PEMS are clearly visible (Fig. 1C, arrowhead marked PEMS). These observations show that cells leaving lRL take two specific pathways: one towards the metencephalon and the other towards the myelencephalon.

Although labelling of more ventrally located regions of the ventricular zone was unavoidable, careful examination of the cases in which the gene transfer was dislocated ventrally revealed the presence of few labelled cells occupying either the AEMS or the PEMS (data not shown). The lRL is therefore the major source of neurons migrating in the AEMS/PEMS.

EYFP-labelled cells migrated immediately beneath the pial surface (Fig. 1D,E, left panels). These observations, together with those from whole-mount preparations, strongly suggest that the labelled cells are PC neurons. To characterize the EYFP-labelled cells further, we examined the expression of *Mbh2/Barhl1*, a Bar-class homeobox gene expressed by PC neurons that project mossy fibres, and disruption of *Mbh2* causes malformation of PC nuclei (Li et al., 2004). We found that *Mbh2* was expressed by most of the EYFP-labelled cells in the AEMS (Fig. 1D) and PEMS (Fig. 1E).

## Migration and subsequent nuclear formation of ECN/LRN neurons

### EYFP-labelled cells in the PEMS migrate across the midline

We observed midline crossing of future ECN/LRN neurons, consistent with previous observations (Bourrat and Sotelo, 1990; Altman and Bayer, 1987a). At E14.5, many EYFP-labelled cells were found in the ipsilateral myelencephalon, migrating tangentially along the dorsal rim of the myelencephalon (Fig. 2A; $n$=12); they had extended leading processes and were aligned in an orderly fashion, forming several thin layers (Fig. 2B). In the ventral midline region, some EYFP-labelled cells extended their leading processes towards the contralateral side (Fig. 2C and inset). These morphological features, together with the absence of labelled cells occupying other regions on the contralateral side, demonstrate that these cells cross the midline.

At this stage, EYFP-labelled neurons did not form aggregates on their ipsilateral migratory route. However, clustered expression of *Mbh2* signal was recognized in the LRN region (Fig. 2D). This is probably due to early-born LRN neurons originating from the contralateral lRL, and suggests that mechanisms for nucleogenesis already operate at this stage. Therefore, the failure of ipsilaterally migrating EYFP-labelled neurons to form aggregates in this location (Fig. 2D) may be due to immaturity of these migrating neurons, rather than to underdeveloped environmental cues required for nucleogenesis.

### A change in migratory directions from tangential to radial

Between E15.5 and E16.5, clusters of labelled cells formed in two distinct regions of the contralateral medulla corresponding to the ECN and LRN (Fig. 2E,G; $n$=12) (Altman and Bayer, 1987a). Some of the cells in these clusters were found some distance beneath the pial surface, and had extended radially oriented processes (Fig. 2F,H). These results show that PC neurons in the PEMS migrate circumferentially, cross the midline and then turn radially at specific locations.

### Morphological maturation and formation of nuclei

We examined these cells at a later stage, E18.5 to study the fate of the EYFP-labelled cells. Fewer EYFP-labelled cells were visible in the PEMS at this stage (data not shown). Conversely, those in the ECN and LRN regions increased in number and occupied a wider area than was observed at E15.5 (Fig. 3A-C; $n$=10). Many of the labelled cells in the deeper regions of these nuclei had multipolar shapes with several processes that resembled dendrites (the left panels of Fig. 3D-F), implying that lRL-derived ECN and LRN precursors are nearly mature as they migrate deep into the medulla.

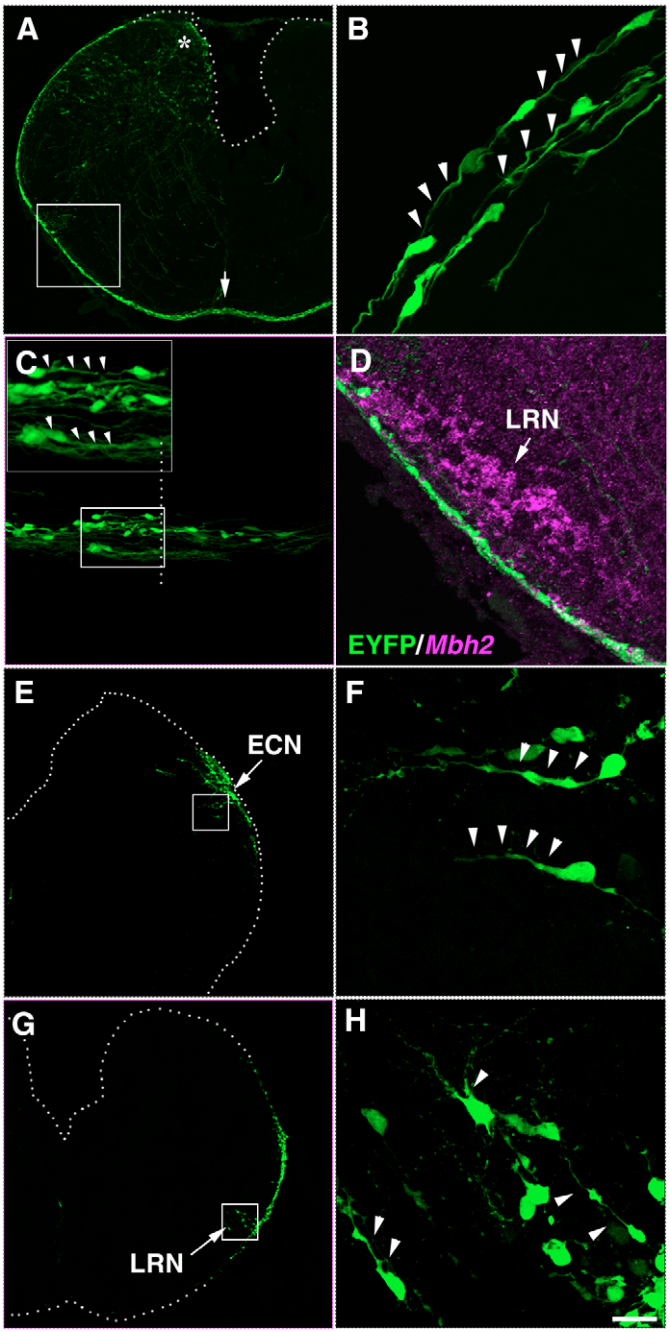


**Fig. 2. Midline crossing and onset of nucleogenesis in the myelencephalon.** (**A**) EYFP-labelled cells migrated tangentially towards the ventral midline (arrow) from the lRL (asterisk). (**B**) EYFP-labelled cells in the dorsal myelencephalon on the side ipsilateral to the injection. Labelled neurons that had left the lRL migrated along the dorsal margin (arrowheads). (**C**) EYFP-labelled neurons found near the ventral midline. The inset shows a higher-power view of the area outlined by the rectangle in C. Many labelled cells cross the ventral midline (arrowheads in the inset). Broken line indicates the midline. (**D**) A higher-power view of the area outlined by the rectangle in A. EYFP-labelled neurons do not form an aggregate ipsilaterally, although cells that appear to originate from the contralateral side as judged by *Mbh2* expression do so. A-D are from E14.5 animals. (**E-H**) The direction of the EYFP-labelled cell migration in the regions of ECN (E) and LRN (G) changed from tangential to radial, with F and H showing higher-magnification views of the areas outlined in E and G, respectively. At E15.5, some of the labelled cells had begun to migrate radially (F,H), extending leading processes (arrowheads in F and H), and had aggregated within the ECN (arrow in E) and LRN (arrow in G). In each panel, *EYFP* was introduced into the left side. Dorsal is upwards. Scale bar: 200 μm for A,E,G; 50 μm for C,D; 25 μm for the inset in C; 20 μm for B,F,H.

To verify that these clusters of EYFP-labelled cells are ECN and LRN neurons, we examined the expression of *Mbh2* mRNA. At E18.5, the labelled neurons were present in a location corresponding to the ECN (Fig. 3A), and in two mediolaterally separated regions that appeared to correspond to the parvocellular and the magnocellular portions of the LRN (Fig. 3B,C) (Bourrat and Sotelo, 1990; Walberg, 1952; Kapogianis et al., 1982). Most of these cells in the dorsal cluster and those in the ventral medulla expressed *Mbh2* (the right panels of Fig. 3D-G). Although labelled cells were also found ipsilaterally, in regions corresponding to the ECN and LRN, there were only a few of these cells, and most were *Mbh2* negative (data not shown). These results show that lRL-derived cells generated from E12.5 onwards give rise to ECN and LRN on the contralateral side.

## Ectopic formation of ECN and LRN by introduction of a dominant negative form of cadherins

Migrating ECN/LRN neurons show a transition in their direction of migration at a specific point along their migratory pathway, raising the possibility that these neurons may recognize cue(s) for the transition. A question then arises of why they do not show a transition on the ipsilateral side. As we discussed above, it seems unlikely that this is due to underdeveloped environmental cues (Fig. 2D).

An alternative possibility is that these neurons acquire competence to respond such presumptive cues depending on the time after their generation. As a tool to test this possibility, we used a dominant-negative form of cadherins [*EGFP-Ncad(t)*], which slows down migration of PC neurons (H.T., D.K., K. Nishida and F.M., unpublished). In E18.5 control preparations, most strong Venus signals were observed in the contralateral ECN and LRN region (Fig. 4A,B). By contrast, when *EGFP-Ncad(t)* was co-electroporated with *Venus*, a large number of *EGFP-Ncad(t)*-transfected neurons appeared to form aggregates in ECN and LRN regions on the ipsilateral side (Fig. 4C,D; $n$=9/12). In transverse sections, we found that many Venus-labelled cells formed clusters in deeper regions of ECN and LRN (Fig. 4E,F; data not shown), intermingled with *Mbh2* signals that may presumably represent the neurons of contralateral origin (insets in Fig. 4E). These observations suggest the possibility that the neurons whose migration was delayed by transfection of *EGFP-Ncad(t)* could recognize the presumptive cues for transition to radial direction on the ipsilateral side and are consistent with the interpretation that ECN and LRN neurons normally acquire responsiveness to the cues depending on an intrinsic, age-dependent mechanism. Moreover, these results indicate that midline crossing of ECN and LRN neurons is not prerequisite for nucleogenesis by these neurons.

## PGN and RTN neurons undergo partial midline crossing and radial migration

Although the midline crossing of PGN and RTN neurons has not been described previously, we did observe midline crossing of EYFP-labelled cells. Fig. 5A shows EYFP-labelled cells in the pons

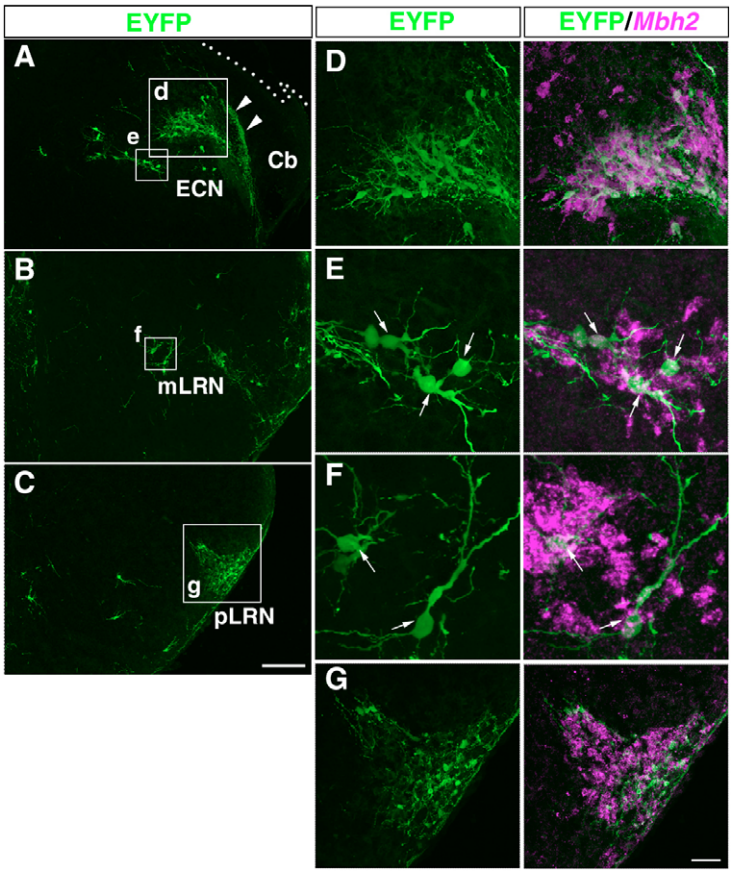


**Fig. 3. Maturation of ECN and LRN.** (**A-C**) The distribution of EYFP-labelled neurons at the level of ECN (A), rostral LRN (B) and caudal LRN (C). Many labelled cells are located in deeper regions of the myelencephalon. Arrowheads in A indicate axons of presumptive LRN neurons. (**D-G**) Transverse sections of E18.5 mice myelencephalon after immunostaining for EYFP (green) and *Mbh2* in situ hybridization (purple). Medial is towards the left and dorsal is upwards. Higher-magnification views of the regions marked d-g. EYFP-labelled cells extended several dendrite-like processes that indicated maturation and expressed *Mbh2* mRNA (the right panels). Arrows in each of the two panels in E and F indicate the same cells. *EYFP* was electroporated into the left lRL. Cb, cerebellum; mLRN, magnocellular part of LRN; pLRN, parvocellular part of LRN. Scale bars: in C, 200 μm for A-C; in right panel of G, 50 μm for D,G and 20 μm for E,F.

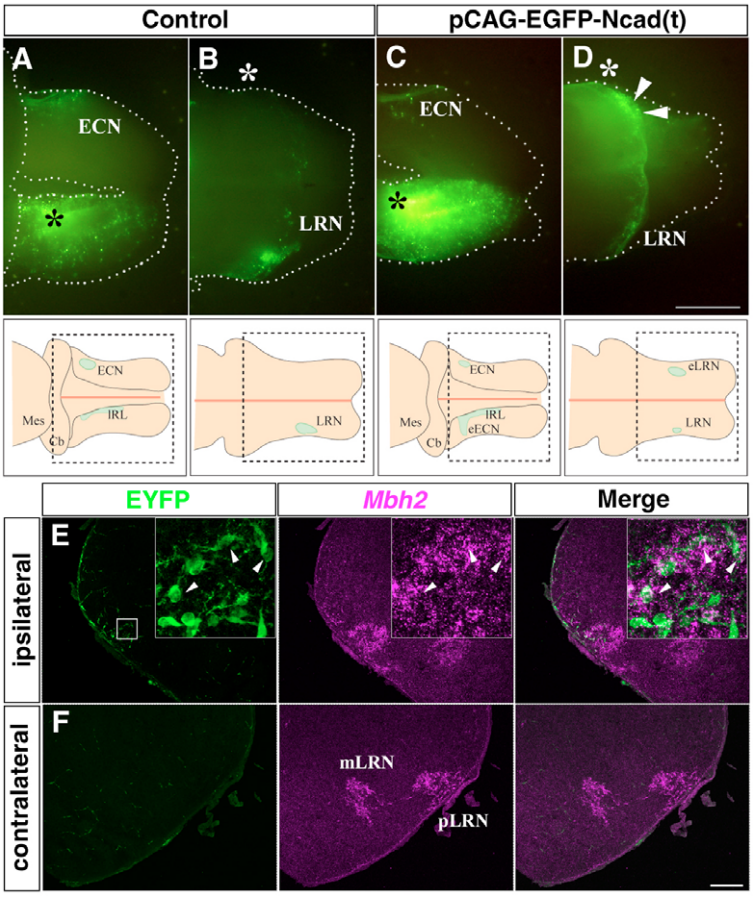


**Fig. 4. Ectopic formation of ECN and LRN caused by dominant-negative form of cadherins.** (**A-D**) Dorsal (A,C) and ventral (B,D) views of E18.5 hindbrains (outlined) labelled by electroporation of pCAG-Venus (A,B) and a mixture of pCAG-Venus and pCAG-EGFP-Ncad(t) (C,D). Although control plasmid (*Venus*) did not affect nucleogenesis of ECN (A) and LRN (B), *EGFP-Ncad(t)* caused an increase in the size of ipsilateral aggregates (arrowheads in D). Asterisks indicate the labelled side. Rostral is towards the left. Areas outlined in lower panels of A-D correspond to the region shown in the upper panels. (**E**,**F**) Localization of *EGFP-Ncad(t)*-transfected cells (left panel) and *Mbh2* signal (middle panel) in ipsilateral (E) and contralateral (F) LRN on transverse section of an E18.5 mouse. Many labelled cells were found in the ipsilateral but not in the contralateral LRN. Neurons in ectopic (ipsilateral) LRN (eLRN) expressed *Mbh2* and were intermingled with untransfected LRN neurons (Venus$^{-}$/*Mbh2*$^{+}$) (right panel of E). Each of the three panels in E and F shows the same field. Insets in E are higher-magnification views of the area outlined in the left panel. eECN, ectopic ECN; eLRN, ectopic LRN. Scale bar: in D, 1mm for A-D; in F, 200 μm for E,F, and 50 μm for insets of E.

of an E14.5 embryo. A substantial number of EYFP-labelled cells had apparently migrated across the ventral midline (broken line) ($n$=12). At E15.5, cells that appeared to have crossed the midline were dispersed dorsally (Fig. 5B, $n$=12).

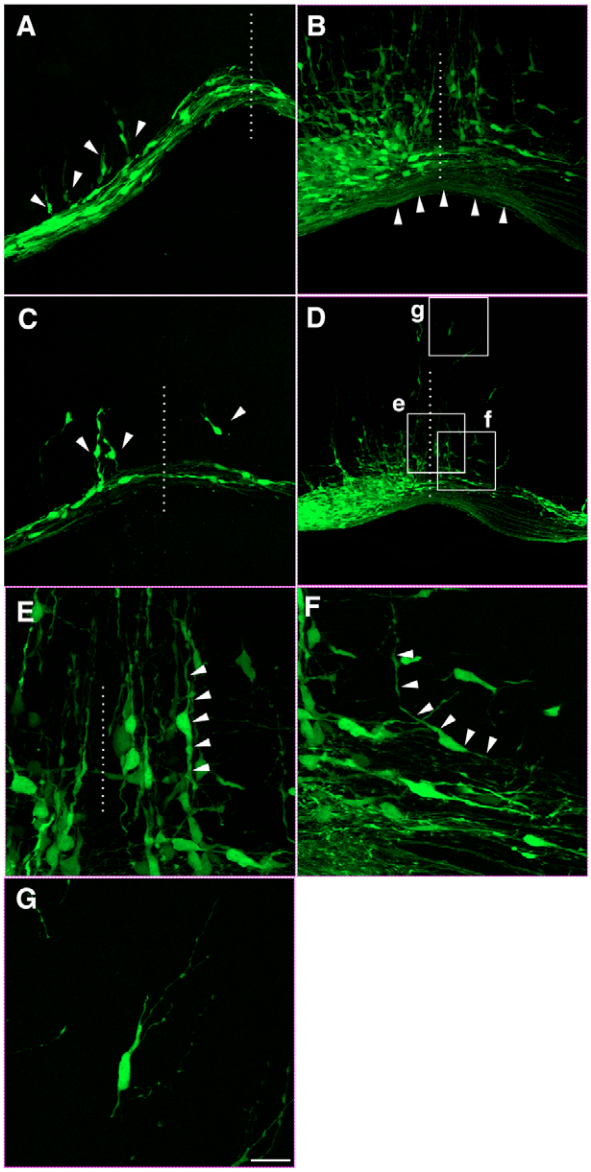


**Fig. 5. Midline crossing and ventricle-directed migration of PGN and RTN neurons.** (**A**) EYFP-labelled cells tangentially migrating across the midline of the pons in an E14.5 mouse. Arrowheads indicate radially deflected cells. (**B**) At E15.5, some EYFP-labelled cells accumulated on the ipsilateral side, while some others were still crossing the midline. (**C**) EYFP-labelled cells that had turned to become ventricle orientated before (arrowheads on the left) and after (arrowhead on the right) midline crossing. E14.5. (**D**) Labelled cells within the pons. E15.5. (**E-G**) High-power views of the rectangular areas marked e-g in D. Ventricle-directed neurons extended a trailing and a leading process (arrowheads in E and F). (F) A cell that had just changed its migratory direction from tangential to ventricle (arrowheads). (G) An RTN neuron that extended several dendrite-like processes. *EYFP* was electroporated into the left lRL. Transverse sections. Dorsal is upwards. Broken lines in A-E represent the positions of the midline. Scale bar: 50 μm for A-C; 100 μm for D; 20 μm for E-G.

At E14.5, cells with radial orientation were occasionally encountered (arrowheads in Fig. 5A,C; $n$=12). By E15.5, such cells were more numerous and found at various distances from the midline on both sides of the neural tube (Fig. 5D, $n$=12). These cells had a typical spindle-shaped morphology, and extended leading and trailing processes (Fig. 5E,F). Cells that had already reached the position of the RTN had extended dendrite-like, branched processes (Fig. 5G). Thus, the cells migrating in the AEMS also change their migration from a tangential to radial direction, on both sides of the neural tube, before they mature.

At E18.5, EYFP-labelled cells formed bilateral clusters that appeared to correspond to the PGN and the RTN. Rostrally, EYFP-labelled cells appeared to occupy the entire territory of the ipsilateral PGN (Fig. 6A,E, $n$=10). However, they were largely confined to the dorsal aspect in the contralateral PGN (Fig. 6A), and axonal profiles, perhaps from the ipsilateral PGN neurons, were found (arrowheads in Fig. 6F) in the ventral pons. Caudally, at the level of the RTN, radially migrating EYFP-labelled neurons were nearly symmetrically distributed on both sides (Fig. 6C, $n$=10). Such ventricle-directed neurons were found in the PGN and RTN, and these cells had several branched processes (Fig. 6G-J) that appeared to be immature dendrites. These results indicate that nucleogenesis by EYFP-labelled cells takes place in the PGN and RTN regions on both sides of the neural tube. EYFP-labelled neurons largely coincided with *Mbh2* (Fig. 6A-D,G-J), further supporting the conclusion that these bilateral clusters of EYFP-labelled cells are PGN and RTN neurons.

## Birthdate-dependent midline crossing of PGN/RTN neurons

The PGN neurons that crossed the midline were found in the dorsal PGN (Fig. 6A,C). Because earlier-generated PGN neurons are located in deeper regions of the hindbrain (Altman and Bayer, 1987b; Altman and Bayer, 1997), it is possible that only the early-born PGN neurons can cross the midline. To test this hypothesis, BrdU was injected at E12.5, E13.5 and E14.5, into pregnant dams that had been electroporated with *EYFP* at E12.5 (Fig. 7). At E18.5, about one-third of the EYFP-positive neurons on the contralateral side were BrdU positive in embryos injected with BrdU at E12.5 (Fig. 7A,C). However, only a few EYFP/BrdU double-positive neurons were observed following BrdU injection at E14.5 (Fig. 7B,D). Most E14.5-born RTN neurons did not express EYFP on the contralateral side (Fig. 7B). Counts of BrdU-labelled cells showed that less than 3% of the EYFP-positive neurons generated at E14.5 reached the contralateral side, compared with more than 30% for the neurons born at E12.5 (Fig. 7E). Therefore, it is the earlier (before E14.5)-generated PGN and RTN neurons that cross the midline.

## Radial fibres may serve as a substrate for ventricle-directed migration of PC neurons

As pial surface-directed radial migration occurs along the radial fibres in the cerebral cortex (Rakic, 1990), we next investigated whether the ventricle-directed migration of PC neurons also takes place along radial fibres. At E15.5, some EYFP-labelled cells in the myelencephalon became ventricle oriented (Fig. 8A,C). The radially extending fibres that span the wall of the hindbrain were immunopositive for nestin, a marker for radial glia-like neuroepithelial cells (Lendahl et al., 1990; Mignone et al., 2004) (Fig. 8C, middle panel). The leading processes of ventricle-oriented ECN and LRN neurons were closely apposed to nestin-positive fibres (data not shown and Fig. 8C, right; $n$=10 cells in 10 slices from three embryos for

ECN, $n$=9 cells in four slices from two embryos for LRN). Ventricle-directed PGN and RTN neurons in the ventral metencephalon were also closely associated with nestin-positive radial fibres (Fig. 8B,D) ($n$=14 cells in three slices from two embryos).

Electron microscopic observations of the pontine region confirmed that cells that appear to be PC neurons directly contacted radially aligned fibres. At a low magnification, radial fibres could be readily recognized by their long and radial extension and their termination at the pial surface (Fig. 8E,F and data not shown). At a high magnification they were characterized by the presence of glycogen particles (arrows in Fig. 8F) (Gadisseux et al., 1990). Presumptive PC neurons could also be recognized by their relatively dark and ribosome-rich cytoplasm (Fig. 8E,F) (Ono and Kawamura, 1990). Consistent with light microscopic observations described above, such cells were oriented both tangentially and towards the ventricle. We examined whether PC cells make contact with radial fibres. As illustrated in Fig. 8F, we occasionally observed a contact between radial fibres and cell bodies of presumptive PC neurons. Contacts between ribosome-rich thin processes which appear to be the leading or trailing process of PC neurons and radial fibres were also encountered (data not shown). Altogether, these results strongly support the conclusion that nestin-positive radial fibres in the hindbrain mediate the ventricle-directed radial migration of PC neurons.

## DISCUSSION

By using exo utero electroporation of *EYFP* into the lRL of mouse embryo, we have visualized the processes of nucleogenesis of four PC nuclei and determined the laterality of their origin. Nucleogenesis of PC neurons involves several migration phases: (1) a sorting into the appropriate migratory route; (2) the tangential migration along the circumferential axis; (3) changes in direction at defined regions; (4) ventricle-directed migration contacting with radial fibres; and (5) termination (Fig. 9). Thus, nucleogenesis is a consequence of precisely regulated successively occurring multi-phasic neuronal migration.

### Identification of EYFP-labelled cells

Our observations that *Mbh2* is expressed by EYFP-positive cells strongly suggest that these cells are PC neurons. *Mbh2* is expressed in the rhombic lip early in development (Bulfone et al., 2000), and its expression pattern corresponds to the anatomically defined

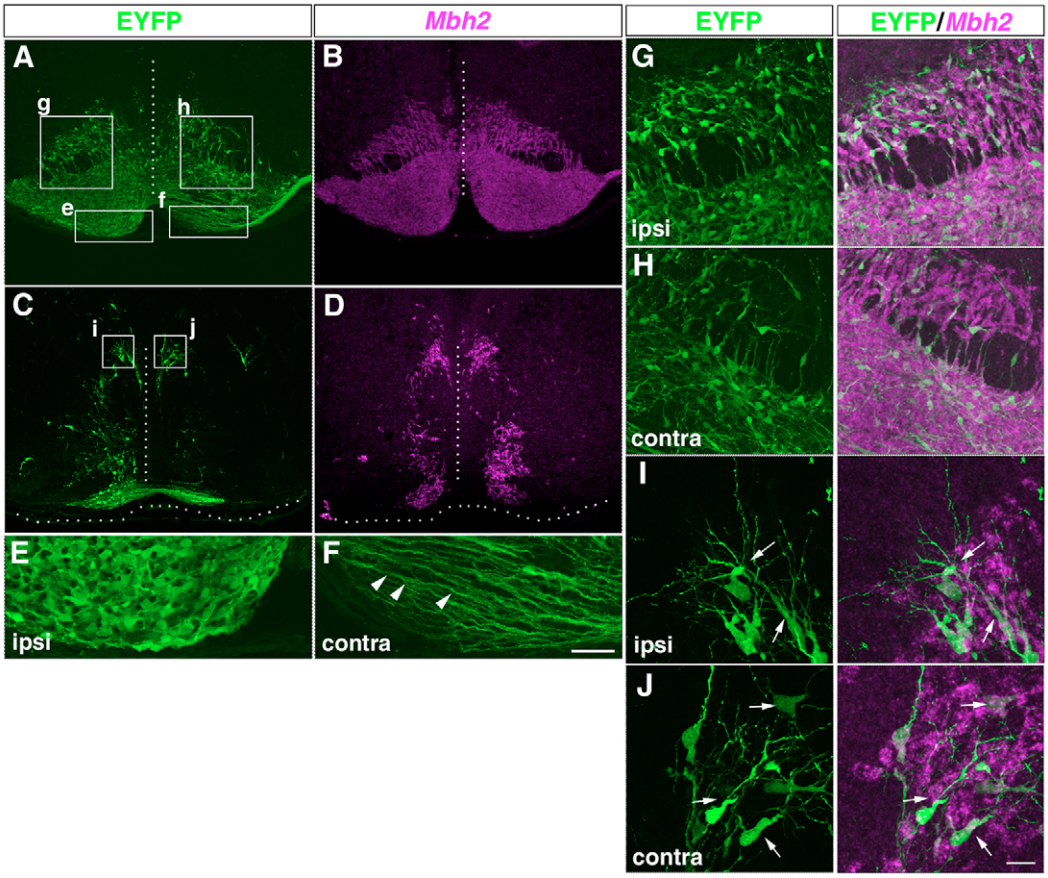


**Fig. 6. Expression of *Mbh2* by EYFP-labelled cells that form clusters in the pons at E18.5.** (**A-D**) EYFP-labelled cells at the level of the rostral (A,B) and caudal (C,D) pons. (B,D) *Mbh2* expression in locations corresponding to A and C. PGN neurons located on the contralateral side were distributed only in the dorsal PGN (A), although RTN neurons were symmetrically distributed on both sides (C). (**E-J**) Higher-power views of the area outlined by rectangles e-j. Although the ventral region of the ipsilateral PGN was densely occupied by labelled cells (E), the corresponding region in the contralateral PGN contained axons (F, arrowheads). Most labelled neurons on both ipsilateral (G,I) and contralateral (H,J) sides expressed *Mbh2* (G-J, right). Arrows in each panel of I and J indicate identical areas. (A,C,E,F) Immunostaining for EYFP; (B,D) *Mbh2* in situ hybridization signals. (G-J) Immunostaining for EYFP (green) and *Mbh2* in situ hybridization pattern (purple) in the same section. *EYFP* was electroporated into the left lRL. E18.5 mouse transverse sections. Dorsal is upwards. Scale bars: in F, 200 μm for A-D and 50 μm for E,F; in J, 50 μm for G,H and 20 μm for I,J.

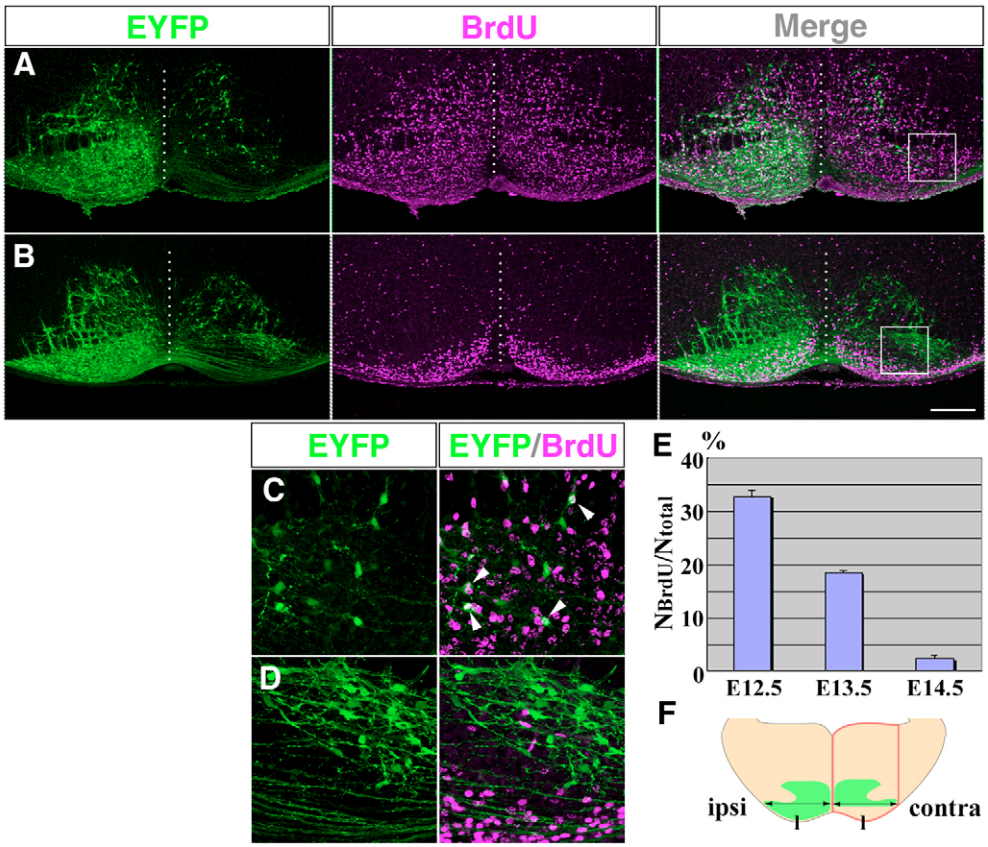


**Fig. 7. Midline crossing of early-born PGN/RTN neurons.** (**A**,**B**) EYFP-expressing PGN/RTN neurons (left panels) labelled with BrdU (middle panels). Right panels show merged views. BrdU was injected at E12.5 (A) or 14.5 (B). Transverse sections of the metencephalon from E18.5 mice. (**C**,**D**) High-power views of the area outlined by rectangles in A,B. Neurons labelled by *EYFP*-electroporation at E12.5 were also labelled by BrdU (white, arrowheads in the right panel of C) when BrdU had been injected at E12.5 (A,C, purple), but not at E14.5 (B,D, purple). E14.5 BrdU injection labelled EYFP-expressing cells occupying the ventral region of the ipsilateral PGN (right panel of B). (**E**) Quantification of BrdU labelling. Ordinate represents the number of BrdU-positive and EYFP-expressing cells ($N_{BrdU}$) divided by the number of EYFP-expressing cells ($N_{total}$) in the contralateral pontine region. The day of BrdU injection is shown along the *y*-axis. Vertical bar represents s.e.m. Each column represents pooled data from five different embryos. (**F**) Diagram showing the quantification method. The mediolateral extent of the PGN (l) was defined as the distance from the midline to the lateral end of the PGN, as visualized by EYFP labelling on the ipsilateral side. All EYFP-labelled cells located within this distance from the midline on the contralateral side (i.e. the region shown by the red contour) were counted. The labelled side is towards the left. Both heavily and lightly labelled cells, in the region described in F, were counted for the analysis. Broken vertical lines in A and B show the midline. Scale bar: 200 μm for A,B; 50 μm for C,D.

positions of mossy-fibre-projecting PC neurons (Li et al., 2004). The axons of EYFP-positive cells, in our embryos examined at E16.5 and later, projected to the cerebellum (D.K., T.S. and F.M., unpublished), which further strengthens the hypothesis that the EYFP-labelled cells are future PC neurons.

*EYFP*-electroporation did not label other PC nuclei, such as the inferior olivary and vestibular nuclei, which also originate from the lRL (Rodriguez and Dymecki, 2000; Altman and Bayer, 1997). This may be largely because the neurons in these nuclei are generated before E12.5 (Taber-Pierce, 1973), and have left the lRL by the time of our electroporation, although there is the possibility that inferior olivary neurons have a distinct origin (Wang et al., 2005; Landsberg et al., 2005).

## Midline crossing of future PC neurons

Previous in vitro studies that labelled presumptive ECN/LRN cells with DiI injections (Kyriakopoulou et al., 2002) or *EGFP* electroporation (Taniguchi et al., 2002) demonstrated migration across the midline. In this study, we have corroborated these findings by providing in vivo evidence that future ECN and LRN neurons originate from the contralateral lRL. Consistent with our results, a recent analysis of *Rig1*-deficient mice implied midline crossing of these neurons (Marillat et al., 2004). An unexpected finding was that a subset of PGN and RTN neurons have a contralateral origin (Figs 5, 6).

## Possible mechanisms involved in tangential migration of PC neurons

There are several important phases in the nucleogenesis of PC neurons. LRL-derived neurons must first determine which of the two migratory pathways they should take (Fig. 1). A recent study demonstrated that *Mbh1/Barhl2*, a homolog of *Mbh2* (Saito et al., 1998), is expressed in AEMS, but not in PEMS (Mo et al., 2004). It is therefore possible that lRL-derived neurons use cues under the control of *Mbh1* when choosing one of these migratory pathways.

We have found that tangential migration of PC neurons is terminated by the transition to ventricle-directed migration, not merely by ceasing to migrate along their tangential route. The

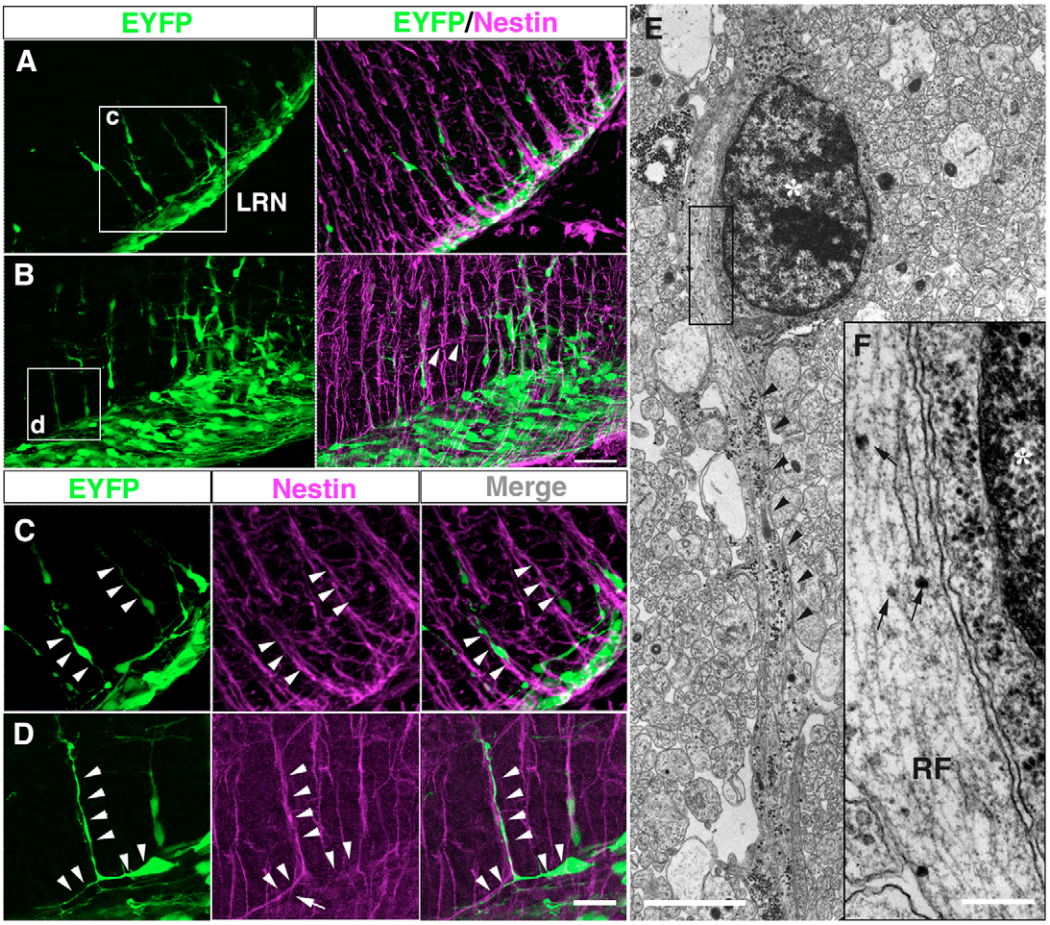


**Fig. 8. EYFP-labelled neurons show ventricle-directed migration in close apposition to nestin-positive radial fibres.** (**A,B**) EYFP-labelled cells (left panels) in the myelencephalon (A) and the metencephalon (B). Subsets of migrating EYFP-labelled PC neurons associated with nestin-positive fibres (purple). Some nestin-positive fibres also extended horizontally (arrowheads in B). (**C,D**) Left panels in C and D show higher-magnification views of the rectangular areas in A and B, respectively. Middle panels show nestin immunostaining. Arrowheads indicate radially extending leading processes of EYFP-labelled neurons apposed to nestin-positive fibres (middle panels) in the myelencephalon (C) and metencephalon (D). An arrow in the middle panel of D shows a tangentially extending fibre. An EYFP-labelled neuron in the pontine region (green) extended branched leading processes that were oriented tangentially and radially, with both branches closely apposed to nestin-positive fibres (arrowheads in right panel of D). *EYFP* was electroporated into the left lRL. (**E,F**) Electron micrographs, taken in the pontine region, of a presumptive PC neuron making contact with a radial fibre (arrowheads in E). F represents higher-magnification view of the rectangle in E. Asterisks in E and F indicate the nucleus of the neuron. The neuron contacts the radial fibre along a length of its plasma membrane. Transverse sections of E15.5 embryos. Right panels in A-D show a merged view with nestin immunostaining of the same section. The ventricle is upwards; the pia is downwards. LRN, lateral reticular nucleus; RF, radial fibre. Scale bars: in B, 50 μm for A,B; in D, 35.2 μm for C and 20 μm for D; in E, 2 μm; in F, 250 nm.

transition and turning could be regulated either by an intrinsic or an extrinsic mechanism. The former is consistent with a previous observation of facial branchiomotor neurons, which regulate expression of surface molecules depending on migration phase (Garel et al., 2000) (for a review, see Chandorasekhar, 2004). However, the fact that the transitions in our study occurred at restricted sites in a protracted period of development during which the size of the neural tube is dramatically increased favours the environmental cue mechanism. Moreover, our results that introduction of *EGFP-Ncad(t)* caused formation of ECN and LRN ipsilaterally but in appropriate locations support the idea that environmental cues exist that induce radial turning at defined locations along the circumferential axis. An interesting possibility is that the transition involves radial fibres at transition points with distinct properties that induce changes in the migratory behaviour of the PC neurons.

Whatever the nature of the cues, our results using dominant-negative form of cadherins suggested that PC neurons acquire responsiveness to turning cues by a time-dependent mechanism (Fig. 9). In addition, these findings imply that changes in responsiveness to such cues occurs independent of their midline crossing. Thus, the speed of ECN/LRN neurons migration should be precisely regulated for proper nucleogenesis on the contralateral side. Further studies are required to clarify these molecular mechanisms.

## Radial-fibre associated, ventricle-directed radial migration

After the phase of tangential migration, PC neurons start migrating towards the ventricle. The role of radial glial cells as a substrate for pial surface-directed migration of cortical neurons is well documented (Marin and Rubenstein, 2003; Rakic, 1990; Hatten and Mason, 1990). Their role in ventricle-directed migration, however,

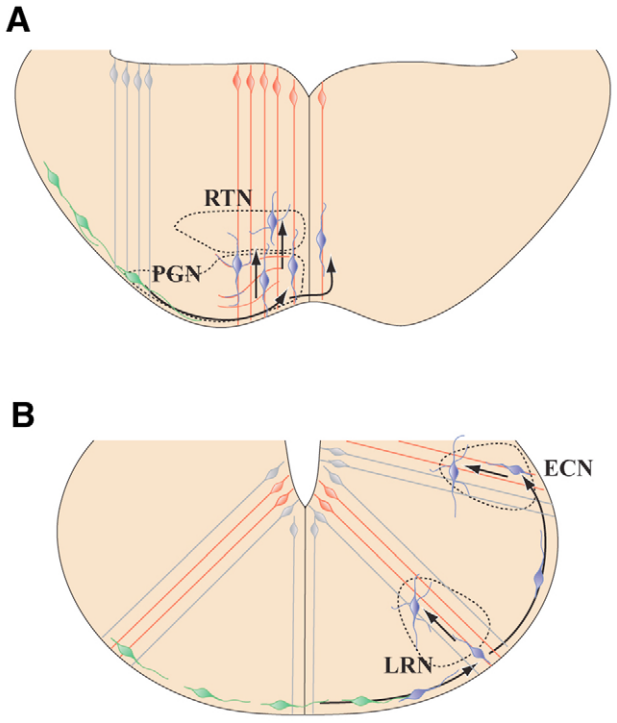


**Fig. 9. Summary diagram showing the process of nucleogenesis by PC neurons.** All subsets of PC neurons show two distinct phases of migration, tangential and radial. (**A**) PGN/RTN neurons first migrate tangentially along the ventral margin of the metencephalon. They then migrate towards the ventricle, either before or after crossing the midline. In this phase, they migrate along nestin-positive radial fibres (red and grey). On arrival at their final destination, they stop migration and extend several dendrite-like processes (violet). In the myelencephalon (**B**), ECN and LRN neurons also initially execute tangential migration and cross the midline. They then migrate along radial fibres towards their final positions, as do PGN/RTN neurons. We hypothesize that PC neurons acquire responsiveness to transition-inducing cues expressed by radial fibres in specific locations (shown in red) and this acquisition takes place in a time-dependent manner (see changes in colour of migrating cells from green to dark blue).

is poorly understood. Here, close association of EYFP-labelled neurons with nestin-positive fibres under the light microscope observed here suggests that PC neurons use radial fibres as a substrate for ventricle-directed migration. This view was strongly supported by our electron microscopic observations, which demonstrated a direct contact of a migrating cell with radial fibres (Fig. 8). Our results provide the first compelling evidence that nestin-positive radial fibres may guide embryonic neurons towards the ventricle, which is essential for the formation of nuclei in appropriate positions.

It is likely that these radial fibres are also used for pial surface-directed migration of hindbrain neurons generated at the ventricular surface, raising the possibility that neurons migrating in opposite direction might collide with each other. This seems unlikely, however, because generation of neurons in the hindbrain ventricular zone seems to occur at earlier stages (Y. Tashiro and F.M., unpublished).

Molecular mechanisms for the ventricle-directed radial migration may be distinct from those for pial-surface directed migration, because genes that play crucial roles in pial-surface directed migration of cortical neurons such as cdk5/p35 (Ohshima et al., 1996; Gupta et al., 2003; Hatanaka et al., 2004) and reelin (Ogawa et al., 1995) do not appear to affect the nucleogenesis of mossy-fibre-projecting PC neurons (Ohshima et al., 2002).

## Specification of distinct neuronal cell types in the hindbrain

The mossy-fibre-projecting PC neurons are characterized by an early (E9.5-11.5) expression of some transcription factors (Li et al., 2004; Rodriguez and Dymecki, 2000; Wang et al., 2005), before they leave the lRL, suggesting that they are already specified before they start migration. However, they have distinct migratory pathways and modes of migration, and their eventual positions are dispersed in the hindbrain (Rodriguez and Dymecki, 2000; Wang et al., 2005) (this study). These features cannot be explained simply by the expression of such genes. There must be some mechanism that allows each subset of PC neurons to express different transcription factors that control the responsiveness of these neurons to environmental cues. To fully understand the molecular mechanisms involved in the development of distinct cell types of PC neurons at specific locations in the hindbrain, the factors that may be involved in the regulation of PC neuron migration remain to be investigated. Our results may help in unravelling the mechanisms underlying these events.

We thank Dr Y. Hatanaka for advice on exo utero electroporation; M. Iwashita for instructions on mouse surgery; Dr J. Miyazaki for a CAG promoter; Dr A. Miyawaki for Venus; Drs N. Yamamoto, H. Kobayashi and Y. Zhu for reading of the manuscript; and Drs K. Nishida, Y. Tashiro and D. Tanaka for discussion and continuous encouragement. Rat 401 antibody was obtained from Developmental Studies Hybridoma Bank, Iowa University. This work was supported by SORST, JST and a Grant-in-Aid for Scientific Research on Priority Area and Advanced Brain Science Project from MEXT(17023028).

### References

**Agarwala, S. and Ragsdale, C. W.** (2002). A role for midbrain arcs in nucleogenesis. *Development* **129**, 5779-5788.
**Altman, J. and Bayer, S. A.** (1987a). Development of the precerebellar nuclei in the rat: III. The posterior precerebellar extramural migratory stream and the lateral reticular and external cuneate nuclei. *J. Comp. Neurol.* **257**, 513-528.
**Altman, J. and Bayer, S. A.** (1987b). Development of the precerebellar nuclei in the rat: IV. The anterior precerebellar extramural migratory stream and the nucleus reticularis tegmenti pontis and the basal pontine gray. *J. Comp. Neurol.* **257**, 529-552.
**Altman, J. and Bayer, S. A.** (1997). In *Development of Cerebellar System in Relation to its Evolution, Structure, and Functions*, pp. 266-321. Boca Raton, FL: CRC Press.
**Angevine, J. B. and Sidman, R. L.** (1961). Autoradiographic study of the cell migration during histogenesis of cerebral cortex in the mouse. *Nature* **192**, 766-768.
**Berry, M. and Rogers, A. W.** (1965). The migration of neuroblasts in the developing cerebral cortex. *J. Anat.* **99**, 691-709.
**Bielas, S., Higginbotham, H., Koizumi, H., Tanaka, T. and Gleeson, J. G.** (2004). Cortical neuronal migration mutants suggest separate but intersecting pathways. *Annu. Rev. Cell Dev. Biol.* **20**, 593-618.
**Bourrat, F. and Sotelo, C.** (1990). Migratory pathways and selective aggregation of the lateral reticular neurons in the rat embryo: a horseradish peroxidase in vitro study, with special reference to migration patterns of the precerebellar nuclei. *J. Comp. Neurol.* **294**, 1-13.
**Bulfone, A., Menguzzato, E., Broccoli, V., Marchitiello, A., Gattuso, C., Mariani, M., Consalez, G. G., Martinez, S., Ballabio, A. and Banfi, S.** (2000). Barhl1, a gene belonging to a new subfamily of mammalian homeobox genes, is expressed in migrating neurons of the CNS. *Hum. Mol. Genet.* **9**, 1443-1452.
**Chandrasekhar, A.** (2004). Turning heads: development of vertebrate branchiomotor neurons. *Dev. Dyn.* **229**, 143-161.
**Gadisseux, J. F., Kadhim, H. J., van den Bosch de Aguilar, P., Caviness, V. S. and Evrard, P.** (1990). Neuron migration within the radial glial fiber system of the developing murine cerebrum: an electron microscopic autoradiographic analysis. *Dev. Brain Res.* **52**, 39-56.
**Garel, S., Garcia-Dominguez, M. and Charnay, P.** (2000). Control of the migratory pathway of facial branchiomotor neurones. *Development* **127**, 5297-5307.

**Goulding, M. and Lamar, E.** (2000). Neuronal patterning: Making stripes in the spinal cord. *Curr. Biol.* **10**, R565-R568.
**Gupta, A., Sanada, K., Miyamoto, D. T., Rovelstad, S., Nadarajah, B., Pearlman, A. L., Brunstrom, J. and Tsai, L. H.** (2003). Layering defect in p35 deficiency is linked to improper neuronal-glial interaction in radial migration. *Nat. Neurosci.* **6**, 1284-1291.
**Harkmark, W.** (1954). Cell migrations from the rhombic lip to the inferior olive, the nucleus raphe and the pons; a morphological and experimental investigation on chick embryos. *J. Comp. Neurol.* **100**, 115-209.
**Hatanaka, Y. and Murakami, F.** (2002). In vitro analysis of the origin, migratory behavior, and maturation of cortical pyramidal cells. *J. Comp. Neurol.* **454**, 1-14.
**Hatanaka, Y., Hisanaga, S., Heizmann, C. W. and Murakami, F.** (2004). Distinct migratory behavior of early- and late-born neurons derived from the cortical ventricular zone. *J. Comp. Neurol.* **479**, 1-14.
**Hatten, M. E.** (1999). Central nervous system neuronal migration. *Annu. Rev. Neurosci.* **22**, 511-539.
**Hatten, M. E. and Mason, C. A.** (1990). Mechanisms of glial-guided neuronal migration in vitro and in vivo. *Experientia.* **46**, 907-916.
**Hockfield, S. and McKay, R. D.** (1985). Identification of major cell classes in the developing mammalian nervous system. *J. Neurosci.* **5**, 3310-3328.
**Kapogianis, E. M., Flumerfelt, B. A. and Hrycyshyn, A. W.** (1982). Cytoarchitecture and cytology of the lateral reticular nucleus in the rat. *Anat Embryol (Berl).* **164**, 229-242.
**Komuro, H. and Yacubova, E.** (2003). Recent advances in cerebellar granule cell migration. *Cell Mol. Life Sci.* **60**, 1084-1098.
**Kriegstein, A. R. and Noctor, S. C.** (2004). Patterns of neuronal migration in the embryonic cortex. *Trends Neurosci.* **27**, 392-399.
**Kyriakopoulou, K., de Diego, I., Wassef, M. and Karagogeos, D.** (2002). A combination of chain and neurophilic migration involving the adhesion molecule TAG-1 in the caudal medulla. *Development* **129**, 287-296.
**Landsberg, R. L., Awatramani, R. B., Hunter, N. L., Farago, A. F., DiPietrantonio, H. J., Rodriguez, C. I. and Dymecki, S. M.** (2005). Hindbrain rhombic lip is comprised of discrete progenitor cell populations allocated by Pax6. *Neuron* **48**, 933-947.
**Lendahl, U., Zimmerman, L. B. and McKay, R. D.** (1990). CNS stem cells express a new class of intermediate filament protein. *Cell* **60**, 585-595.
**Li, S., Qiu, F., Xu, A., Price, S. M. and Xiang, M.** (2004). Barhl1 regulates migration and survival of cerebellar granule cells by controlling expression of the neurotrophin-3 gene. *J. Neurosci.* **24**, 3104-3114.
**Marillat, V., Sabztier, C., Failli, V., Matsunaga, E., Sotelo, C., Tessier-Lavigne, M. and Chedotal, A.** (2004). The slit receptor Rig-1/Robo3 controls midline crossing by hindbrain precerebellar neurons and axons. *Neuron* **43**, 69-79.
**Marin, O. and Rubenstein, J. L.** (2003). Cell migration in the forebrain. *Annu. Rev. Neurosci.* **26**, 441-483.
**Mignone, J. L., Kukekov, V., Chiang, A. S., Steindler, D. and Enikolopov, G.** (2004). Neural stem and progenitor cells in nestin-GFP transgenic mice. *J. Comp. Neurol.* **469**, 311-324.
**Mo, Z., Li, S., Yang, X. and Xiang, M.** (2004). Role of the Barhl2 homeobox gene in the specification of glycinergic amacrine cells. *Development* **131**, 1607-1618.
**Nagai, T., Ibata, K., Park, E. S., Kubota, M., Mikoshiba, K. and Miyawaki, A.** (2002). A variant of yellow fluorescent protein with fast and efficient maturation for cell-biological applications. *Nat. Biotechnol.* **20**, 87-90.
**Niwa, H., Yamamura, K. and Miyazaki, J.** (1991). Efficient selection for high-expression transfectants with a novel eukaryotic vector. *Gene* **108**, 193-199.
**Ogawa, M., Miyata, T., Nakajima, K., Yagyu, K., Seike, M., Ikenaka, K., Yamamoto, H. and Mikoshiba, K.** (1995). The reeler gene-associated antigen on Cajal-Retzius neurons is a crucial molecule for laminar organization of cortical neurons. *Neuron* **14**, 899-912.
**Ohshima, T., Ward, J. M., Huh, C. G., Longenecker, G., Veeranna Pant, H. C., Brady, R. O., Martin, L. J. and Kulkarni, A. B.** (1996). Targeted disruption of the cyclin-dependent kinase 5 gene results in abnormal corticogenesis, neuronal pathology and perinatal death. *Proc. Natl. Acad. Sci. USA* **93**, 11173-11178.
**Ohshima, T., Ogawa, M., Takeuchi, K., Takahashi, S., Kulkarni, A. B. and Mikoshiba, K.** (2002). Cyclin-dependent kinase 5/p35 contributes synergistically with Reelin/Dab1 to the positioning of facial branchiomotor and inferior olive neurons in the developing mouse hindbrain. *J. Neurosci.* **22**, 4036-4044.
**Ono, K. and Kawamura, K.** (1990). Mode of neuronal migration of the pontine stream in fetal mice. *Anat. Embryol. (Berl)* **182**, 11-19.
**Rakic, P.** (1972). Mode of cell migration to the superficial layers of fetal monkey neocortex. *J. Comp. Neurol.* **145**, 61-83.
**Rakic, P.** (1974). Neurons in rhesus monkey visual cortex: systematic relation between time of origin and eventual disposition. *Science* **183**, 425-427.
**Rakic, P.** (1990). Principles of neural cell migration. *Experientia* **46**, 882-891.
**Rodriguez, C. I. and Dymecki, S. M.** (2000). Origin of the precerebellar system. *Neuron* **27**, 475-486.
**Saba, R., Nakatsuji, N. and Saito, T.** (2003). Mammalian BarH1 confers commissural neuron identity on dorsal cells in the spinal cord. *J. Neurosci.* **23**, 1987-1991.
**Saito, T., Sawamoto, K., Okano, H., Anderson, D. J. and Mikoshiba, K.** (1998). Mammalian BarH homologue is a potential regulator of neural bHLH genes. *Dev. Biol.* **199**, 216-225.
**Sotelo, C.** (2004). Cellular and genetic regulation of the development of the cerebellar system. *Prog. Neurobiol.* **72**, 295-339.
**Taber-Pierce, E.** (1966). Histogenesis of the nuclei griseum pontis, corporis pontobulbaris and reticularis tegmenti pontis (bechterew) in mouse. *J. Comp. Neurol.* **126**, 219-240.
**Taber-Pierce, E.** (1973). Time of origin of neurons in the brain stem of the mouse. *Prog. Brain Res.* **40**, 53-65.
**Tan, K. and Le Douarin, N. M.** (1991). Development of the nuclei and cell migration in the medulla oblongata. Application of the quail-chick chimera system. *Anat. Embryol. (Berl).* **183**, 321-343.
**Taniguchi, H., Tamada, A., Kennedy, T. E. and Murakami, F.** (2002). Crossing the ventral midline causes neurons to change their response to floor plate and alar plate attractive cues during transmedian migration. *Dev. Biol.* **249**, 321-332.
**Walberg, F.** (1952). The lateral reticular nucleus of the medulla oblongata in mammals; a comparative-anatomical study. *J. Comp. Neurol.* **96**, 283-343.
**Wang, V. Y., Rose, M. F. and Zoghbi, H. Y.** (2005). Math1 expression redefines the rhombic lip derivatives and reveals novel lineages within the brainstem and cerebellum. *Neuron* **48**, 31-43.
**Wingate, R. J.** (2001). The rhombic lip and early cerebellar development. *Curr. Opin. Neurobiol.* **11**, 82-88.